Phase diagram as a function of doping level and pressure in the $Eu_{1-x}La_xFe_2As_2$ system

M. Zhang,[1] J. J. Ying,[1] Y. J. Yan,[1] A. F. Wang,[1] X. F. Wang,[1] Z. J. Xiang,[1] G. J. Ye,[1] P. Cheng,[1] X. G. Luo,[1] Jiangping Hu,[2,3] and X. H. Chen[1,*]

[1]*Hefei National Laboratory for Physical Science at Microscale and Department of Physics, University of Science and Technology of China, Hefei, Anhui 230026, People's Republic of China*

[2]*Beijing National Laboratory for Condensed Matter Physics, Institute of Physics, Chinese Academy of Sciences, Beijing 100190, China*

[3]*Department of Physics, Purdue University, West Lafayette, Indiana 47907, USA*

(Received 14 January 2012; published 14 March 2012)

We establish the phase diagram of the $Eu_{1-x}La_xFe_2As_2$ system as a function of doping level x and pressure by measuring the resistivity and magnetic susceptibility. Increased pressure can suppress the spin-density-wave (SDW) and structural transitions very efficiently, while enhancing the antiferromagnetic (AFM) transition temperature T_N of Eu^{2+}. Superconductivity coexists with SDW order at low pressure and always coexists with Eu^{2+} AFM order. The results suggest that the Eu^{2+} spin dynamics is unconnected with the superconducting pairing taking place in the two-dimensional Fe-As plane, but it can strongly affect superconducting coherence along the c axis.

DOI: 10.1103/PhysRevB.85.092503 PACS number(s): 74.62.Fj, 74.25.fc, 74.25.Ha, 75.30.−m

Iron-based superconductors have attracted great attention in recent years.[1–4] The parent compound undergoes structural and spin-density-wave (SDW) transitions. With chemical doping or high pressure, both the structural and SDW transitions can be suppressed and superconductivity emerges. AFe_2As_2 compounds (A = Ca, Sr, Ba, Eu) with the $ThCr_2Si_2$-type structure have been widely investigated because it is easy to grow large-size, high-quality single crystals.[5] The maximum T_c for hole-doped samples is about 38 K and for Co-doped samples it is about 26 K.[4,6] Recently, superconductivity up to 49 K was discovered in rare-earth-doped $CaFe_2As_2$; it is the highest T_c observed in the 122 system.[7–10] $EuFe_2As_2$ has the same structure as $CaFe_2As_2$.[11] $EuFe_2As_2$ shows superconductivity around 31 K under a pressure of 3 GPa.[12]

The Eu122 system has an interesting outstanding issue regarding the interplay between the magnetism of the large Eu^{2+} spins and the superconductivity. Doping in the Eu122 system has been achieved in two ways: direct electron doping in the Fe-As layer, as in Co-doped Eu122, and doping induced by Eu replacement with other rare-earth atoms, as in $Eu_{1-x}La_xFe_2As_2$. In the former case, a resistivity reentrance due to the antiferromagnetic (AFM) order of the Eu^{2+} spins was often observed,[13–16] an indication of the effect of Eu^{2+} spins on superconductivity. However, a clear understanding of this effect has not been established as a systematic investigation is lacking. In the latter case, earlier results on $Eu_{1-x}La_xFe_2As_2$ show only a gradual decrease of the spin-density-wave transition temperature T_{SDW} of the Fe spins with increasing La content. No superconducting transition was observed[17] and no information regarding the role of Eu^{2+} spins has been provided.

High pressure is confirmed to be a good method to tune the phase competition of superconductivity and SDWs in iron pnicide superconductors. In this Brief Report, we report a systematic investigation of the superconductivity in the La-doped $EuFe_2As_2$ system under ambient and high pressure by resistivity and magnetic susceptibility measurements. We obtain a complete phase diagram. One superconducting transition was observed in the sample of La-doped $EuFe_2As_2$ with the highest doping level, while zero resistivity cannot be reached under ambient pressure. Both the structural and SDW transitions can be completely suppressed and zero resistivity can be achieved under high pressure. An intriguing result is that the antiferromagnetic transition temperature T_N of the local moments of the Eu^{2+} ions is always higher than T_c and is not affected by La doping; it slightly increases with increasing pressure. This suggests that, although superconductivity (SC) always coexists with AFM order of the Eu^{2+} ions, the two types of order are unconnected with each other in La-doped $EuFe_2As_2$. Together with earlier work on Co-doped Eu122,[13–16] these results suggest that Eu^{2+} spins strongly affect SC coherence only along the c axis, but not the SC pairing in Fe-As layers.

High-quality single crystals with nominal composition $Eu_{1-x}La_xFe_2As_2$ (x = 0, 0.15, 0.3, 0.4, 0.5) were grown by conventional solid-state reaction using FeAs as self-flux. Clean Eu bulk, La bulk, Fe powder, and As powder were employed as starting materials. The starting materials were weighed in the stoichiometric ratio inside an Ar-filled glove box. The mixture was loaded into an alumina crucible and then sealed into a quartz tube under vacuum. It was slowly heated to 680 °C, held for 12 h, and then heated to 1170 °C for 10 h; then the quartz tube was cooled to 900 °C at a rate of 4 K/h. Finally, the quartz tube was cooled in the furnace after shutting off the power. The shining platelike $Eu_{1-x}La_xFe_2As_2$ crystals were mechanically cleaved from the flux and obtained for measurements. Energy-dispersive x-ray spectroscopy indicates that the actually doping x was 0, 0.08, 0.15, 0.22, and 0.27 for these five La-doped samples. A problem that remains to be addressed is that the maximum solid-solution value of x to be achieved is 0.27, although the nominal doping level is much larger than 0.5. Pressure was generated in a Teflon cup filled with Daphne Oil 7373 which was inserted into a Be-Cu pressure cell. The resistivity measurements were performed using a Quantum Design physical properties measurement systm (PPMS-9), and magnetic susceptibility was measured using a Quantum Design superconducting quantum intereference device and magnetic properties measurement system.

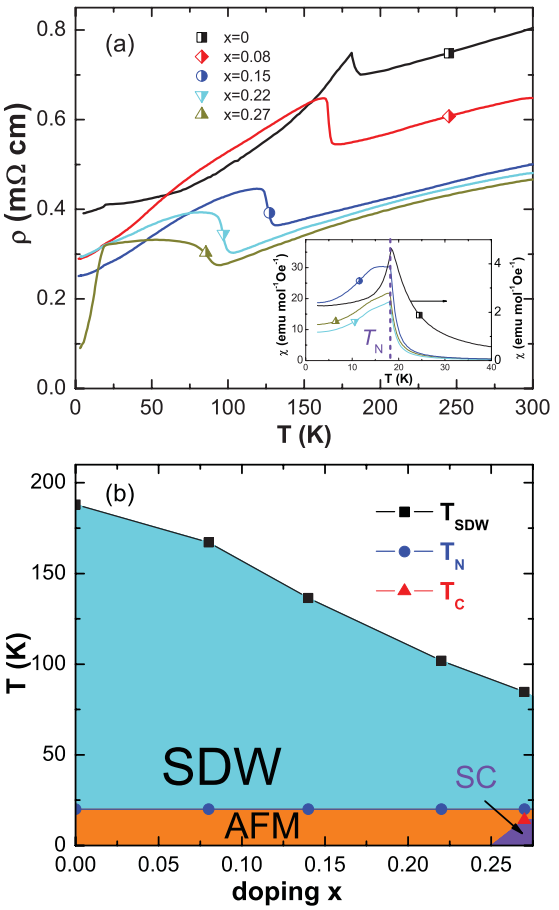

FIG. 1. (Color online) (a) Temperature dependence of resistivity for $Eu_{1-x}La_xFe_2As_2$ with different doping x. The inset shows the temperature dependence of susceptibility below 40 K. (b) The phase diagram of $Eu_{1-x}La_xFe_2As_2$ derived from the resistivity and susceptibility. The label AFM indicates the antiferromagnetic state of Eu^{2+}.

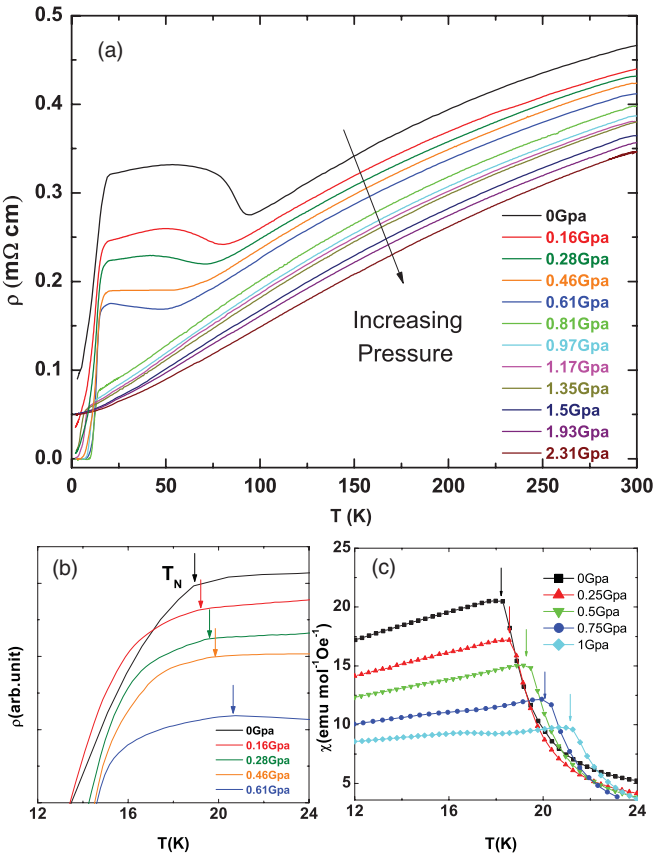

FIG. 2. (Color online) (a) Temperature dependence of resistivity for $Eu_{0.73}La_{0.27}Fe_2As_2$ under different pressures. (b) Magnification of the temperature-dependent resistivity under various pressures around T_N. (c) Magnification of the temperature dependence of susceptibility under various pressures around T_N.

Figure 1(a) shows the temperature dependence of resistivity for the samples of $Eu_{1-x}La_xFe_2As_2$ with different doping levels. For the parent compound, two anomalies in resistivity are observed at 188 and 20 K, respectively. They arise from the SDW and structural transitions and the AFM order of local moments of the Eu^{2+} ions.[17] The resistivity anomaly arising from the the SDW and structural transitions is gradually suppressed with increasing doping x, while the anomaly around 20 K due to the antiferromagnetic transition of Eu^{2+} ions is nearly unchanged by variation of the La doping. The inset shows the temperature dependence of susceptibility for the samples of $Eu_{1-x}La_xFe_2As_2$ with different x. It is found that the antiferromagnetic transition temperature (T_N) does not change although the content of Eu^{2+} is decreased by substitution of the La^{3+}. This behavior in the susceptibility is consistent with that observed in the resistivity. A superconducting transition is observed in the sample with $x = 0.27$; however, zero resistivity cannot be reached. Figure 1(b) shows the phase diagram obtained from the resistivity and susceptibility measurements for the $Eu_{1-x}La_xFe_2As_2$ system. The structural and SDW transitions temperature is suppressed to about 85 K, and superconductivity emerges when the La doping is increased to 0.27. However, the solid-solution x for $Eu_{1-x}La_xFe_2As_2$ cannot be larger than 0.27. Therefore, we cannot obtain the whole phase diagram under ambient pressure in the $Eu_{1-x}La_xFe_2As_2$ system. The phase diagram shows that T_N is nearly independent of the La doping.

In order to obtain a complete phase diagram in the $Eu_{1-x}La_xFe_2As_2$ system, we performed resistivity and susceptibility measurements for the sample with the maximal La doping $x = 0.27$ under hydrostatic pressure. It is well known that the pressure provides another way to suppress SDW order and to induce supercodncutivity; therefore, a complete phase diagram is expected under pressure in the $Eu_{1-x}La_xFe_2As_2$ system. Figure 2(a) shows the temperature dependence of resistivity for the sample with $x = 0.27$. It is found that increasing pressure can suppress both the structural and the SDW transition very efficiently and greatly improves the superconductivity. Zero resistivity is achieved under a pressure of 0.46 GPa. With increasing pressure larger than 0.81 GPa, the structure and SDW transitions are completely suppressed. When the applied pressure is larger than about 1.5 GPa, the superconductivity disappears. As shown in Fig. 2(b), the temperature corresponding to the kink in resistivity due to the AFM order of the Eu^{2+} ions increases with increasing pressure. To confirm the behavior, we also measured the susceptibility with the magnetic field applied under pressure within the

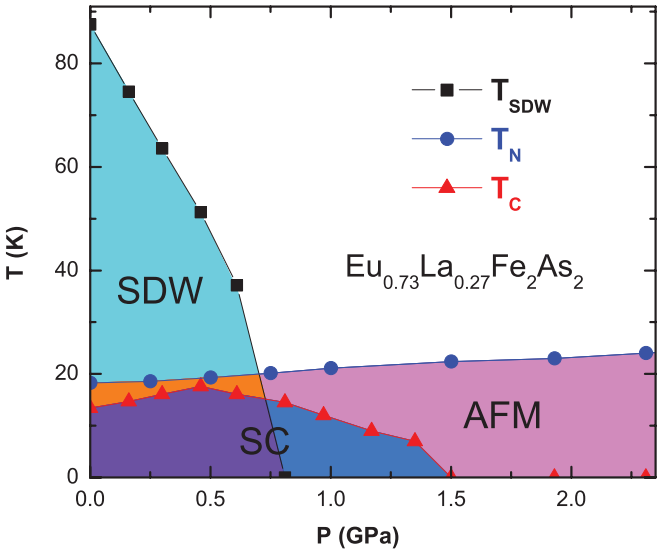

FIG. 3. (Color online) The pressure phase diagram of $Eu_{0.73}La_{0.27}Fe_2As_2$ derived from the resistivity and susceptibility. The label AFM indicates the antiferromagnetic state of Eu^{2+}.

ab plane of the crystal. Figure 2(c) shows the temperature dependence of susceptibility under different pressures. It clearly shows that the temperature of the antiferromagnetic transition slightly increases with increasing pressure, which is consistent with the results from the resistivity measurements.

Based on the results for resistivity and susceptibility under pressure as shown in Fig. 2, a complete phase diagram is obtained, and plotted in Fig. 3. The phase diagram is very complicated and similar to those of $Ba_{1-x}K_xFe_2As_2$ and $BaFe_{2-x}Co_xAs_2$.[18,19] As shown in the phase diagram, the $Eu_{0.73}La_{0.27}Fe_2As_2$ system shows the coexistence of superconductivity and SDWs under pressures below 0.8 GPa. In addition, there exists an antiferromagnetic order arising from the local moment of Eu^{2+} ions. This AFM order occurs at all the various applied pressures. It should be pointed out that T_N is always higher than the T_c. This indicates that the three phases of superconducting, SDW, and AFM order coexist under pressures below 0.8 Gpa. In this sense, the phase diagram is complicated relative to those of $Ba_{1-x}K_xFe_2As_2$ and $BaFe_{2-x}Co_xAs_2$. The superconductivity is completely suppressed under a pressure of 1.5 GPa, much lower than the corresponding pressure in the parent compound $EuFe_2As_2$. This suggests that La doping and pressure have the same effect on the superconductivity and on SDWs. However, increasing pressure can enhance T_N.

We also studied the phase diagram of the sample $Eu_{0.78}La_{0.22}Fe_2As_2$ by measuring the resistivity and susceptibility. Figure 4(a) shows the temperature dependence of resistivity under the various pressure. $Eu_{0.78}La_{0.22}Fe_2As_2$ shows structural and SDW transitions around 96 K and no superconducting transition is detected under ambient pressure. When a small pressure of about 0.5 GPa is applied, the resistivity shows a hint of a superconducting transition, similarly to the case for the sample with $x = 0.27$ under ambient pressure. T_c gradually increases and zero resistivity is achieved with further increase in pressure. When the applied pressure is larger than 0.7 GPa, T_c starts to decrease with increasing

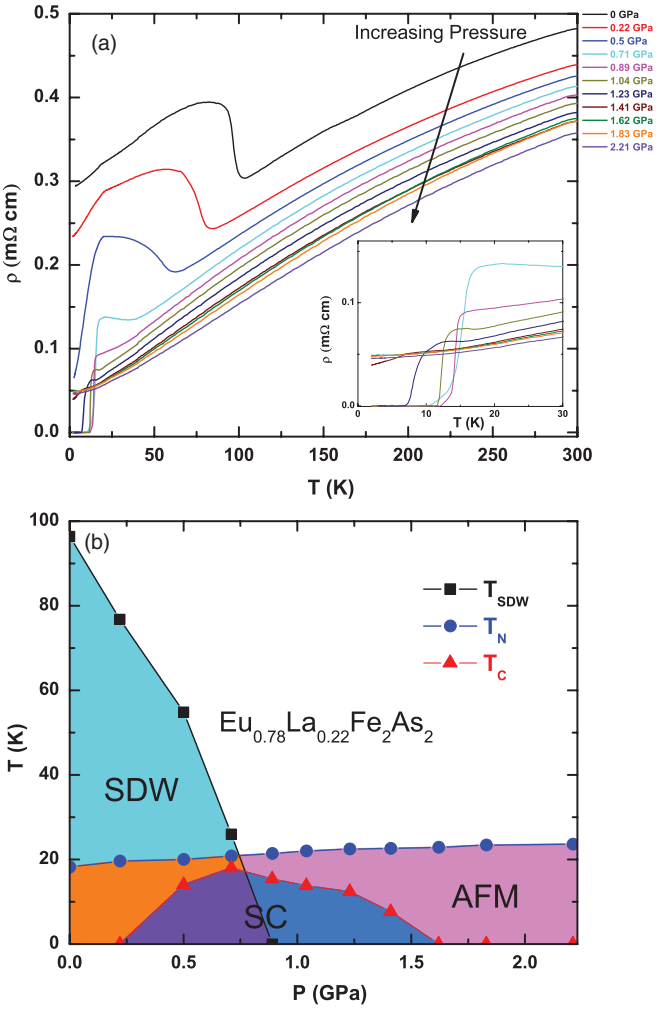

FIG. 4. (Color online) (a) Temperature dependence of resistivity for $Eu_{0.78}La_{0.22}Fe_2As_2$ under different pressures. The inset is a magnification of the resistivity around T_c. (b) The pressure phase diagram of $Eu_{0.78}La_{0.22}Fe_2As_2$ derived from the resistivity and susceptibility. The label AFM indicates the antiferromagnetic state of Eu^{2+}.

pressure, and superconductivity is completely suppressed when pressure up to 1.62 GPa is applied. The resistivity behavior of $Eu_{0.78}La_{0.22}Fe_2As_2$ under low pressure is very similar to that observed in the sample of $Eu_{0.73}La_{0.27}Fe_2As_2$ at ambient pressure. This further indicates that La doping has the same effect on SDW order and superconductivity as applied pressure. The phase diagram of the sample $Eu_{0.78}La_{0.22}Fe_2As_2$ as a function of pressure is plotted in Fig. 4(b). The phase diagram is the same as those with the control parameter x observed in the $Ba_{1-x}K_xFe_2As_2$ and $BaFe_{2-x}Co_xAs_2$ systems except for the existence of AFM order of the Eu^{2+} ions.

Both the structural and SDW transitions are suppressed with increasing La doping only the superconducting transition can be achieved and no zero resistance is reached in the $Eu_{1-x}La_xFe_2As_2$ system. The AFM transition of the Eu^{2+} ions is barely affected by La doping. With application of external pressure, the superconductivity can be improved greatly in the highly-La-doped samples. A SC dome appears in the *T*-*P* phase diagram. However, the AFM transition of Eu^{2+}

is scarcely affected by pressure. These results suggest that the superconductivity is unconnected with the AFM order in the $Eu_{1-x}La_xFe_2As_2$ system.

It is intriguing to compare our results with earlier results on other Eu122 compounds.[16,20–22] In the parent compound $EuFe_2As_2$, T_c is about 31 K under pressure. A resistivity reentrance due to the antiferromagnetic ordering of Eu^{2+} spins is widely observed in other Eu122 systems below T_c.[16,20,21] In $Sr_{1-y}Eu_y(Fe_{0.88}Co_{0.12})_2As_2$ single crystals, Hu *et al.*[22] claimed that the bulk SC disappears suddenly when $T_N > T_c$. These results definitely indicates the strong competition between AFM and SC. Thus, this comparison indicates a dilemma regarding the relation between the AFM and SC.

This dilemma can be easily resolved if we assume that the major effect of Eu^{2+} spins on SC is along the c axis. In a quasi-two-dimensional system, a global SC state is formed only when the SC coherence is reached along the c axis. In La-doped Eu122, the electrons doped into the Fe-As layer stem from La. SC coherence along the c axis can be achieved by virtual hopping through La atoms, which minimizes the effect of the dynamics of Eu^{2+} spins. However, in the parent compounds or Co-doped Eu122, the similar processes go via Eu and the Eu^{2+} spins can strongly affect the SC coherence along the c axis. If the pairing in the Fe-As layer is strong, resistivity reentrance can take place due to the blocking of c-axis coherence by the critical fluctuations of Eu^{2+} spins near the AFM transition, which explains the observed phenomena in the parent compounds of Eu122. If the pairing in the Fe-As layer is weak, phase coherence along the c axis may never develop under the influence of Eu^{2+} spins, which accounts for the observations in in Co-doped Eu122.

In conclusion, by measuring the resistivity and susceptibility under various pressures, we established the complete phase diagram for crystals of $Eu_{1-x}La_xFe_2As_2$ with different x. Only a trace of superconductivity was observed in the highly-La-doped samples under ambient pressure. High pressure efficiently suppresses the SDW and structural transitions and improves the superconductivity; it also leads to an increase in T_N. Superconductivity coexists with SDW order at low pressure, and always coexists with the antiferromagnetic order of the Eu^{2+} spins.

This work is supported by the National Natural Science Foundation of China (Grant No. 51021091), the National Basic Research Program of China (973 Program, Grants No. 2011CB00101 and No. 2012CB922002), and the Chinese Academy of Sciences.

*chenxh@ustc.edu.cn

[1] Y. Kamihara, T. Watanabe, M. Hirano, and H. Hosono, J. Am. Chem. Soc. **130**, 3296 (2008).
[2] X. H. Chen, T. Wu, G. Wu, R. H. Liu, H. Chen, and D. F. Fang, Nature (London) **453**, 761 (2008).
[3] Z. A. Ren, G. C. Che, X. L. Dong, J. Yang, W. Lu, W. Yi, X. L. Shen, Z. C. Li, L. L. Sun, F. Zhou, and Z.X. Zhao, Europhys. Lett. **83**, 17002 (2008).
[4] M. Rotter, M. Tegel, and D. Johrendt, Phys. Rev. Lett. **101**, 107006 (2008).
[5] X. F. Wang, T. Wu, G. Wu, H. Chen, Y. L. Xie, J. J. Ying, Y. J. Yan, R. H. Liu, and X. H. Chen, Phys. Rev. Lett. **102**, 117005 (2009).
[6] A. S. Sefat, R. Jin, M. A. McGuire, B. C. Sales, D. J. Singh, and D. Mandrus, Phys. Rev. Lett. **101**, 117004 (2008).
[7] S. R. Saha, N. P. Butch, T. Drye, J. Magill, S. Ziemak, K. Kirshenbaum, P. Y. Zavalij, J. W. Lynn, and J. Paglione, Phys. Rev. B **85**, 024525 (2012).
[8] Z. S. Gao, Y. P. Qi, L. Wang, D. L. Wang, X. P. Zhang, C. Yao, C. L. Wang, and Y. W. Ma, Europhys. Lett. **95**, 67002 (2011).
[9] B. Lv, L. Z. Deng, M. Gooch, F. Y. Wei, Y. Y. Sun, J. K. Meen, Y. Y. Xue, B. Lorenz, and C. W. Chu, Proc. Natl. Acad. Sci. USA **108**, 15705 (2011).
[10] Y. P. Qi, Z. S. Gao, L. Wang, D. L. Wang, X. P. Zhang, C. Yao, C. L. Wang, C. D. Wang, and Y. W. Ma, e-print arXiv:1106.4208.
[11] Z. Ren, Z. Zhu, S. Jiang, X. Xu, Q. Tao, C. Wang, C. Feng, G. Cao, and Z. Xu, Phys. Rev. B **78**, 052501 (2008).
[12] N. Kurita, M. Kimata, K. Kodama, A. Harada, M. Tomita, H. S. Suzuki, T. Matsumoto, K. Murata, S. Uji, and T. Terashima, Phys. Rev. B **83**, 214513 (2011).
[13] Z. Ren, Q. Tao, S. Jiang, C. Feng, C. Wang, J. Dai, G. Cao, and Z. Xu, Phys. Rev. Lett. **102**, 137002 (2009).
[14] C. F. Miclea, M. Nicklas, H. S. Jeevan, D. Kasinathan, Z. Hossain, H. Rosner, P. Gegenwart, C. Geibel, and F. Steglich, Phys. Rev. B **79**, 212509 (2009).
[15] J. J. Ying, T. Wu, Q. J. Zheng, Y. He, G. Wu, Q. J. Li, Y. J. Yan, Y. L. Xie, R. H. Liu, X. F. Wang, and X. H. Chen, Phys. Rev. B **81**, 052503 (2010).
[16] Y. He, T. Wu, G. Wu, Q. J. Zheng, Y. Z. Liu, H. Chen, J. J. Ying, R. H. Liu, X. F. Wang, Y. L. Xie, Y. J. Yan, J. K. Dong, S. Y. Li, and X. H. Chen, J. Phys.: Condens. Matter **22**, 235701 (2010).
[17] T. Wu, G. Wu, H. Chen, Y. L. Xie, R. H. Liu, X. F. Wang, and X. H. Chen, J. Magn. Magn. Mater. **321**, 3870 (2009).
[18] H. Chen, Y. Ren, Y. Qiu, Wei Bao, R. H. Liu, G. Wu, T. Wu, Y. L. Xie, X. F. Wang, Q. Huang, and X. H. Chen, Europhys. Lett. **85**, 17006 (2009).
[19] X. F. Wang, T. Wu, G. Wu, R. H. Liu, H. Chen, Y. L. Xie, and X. H. Chen, New J. Phys. **11**, 045003 (2009).
[20] T. Park, E. Park, H. Lee, T. Klimczuk, E. D. Bauer, F. Ronning, and J. D. Thompson, J. Phys.: Condens. Matter **20**, 322204 (2008).
[21] P. L. Alireza, Y. T. Chris Ko, J. Gillett, C. M. Petrone, J. M. Cole, G. G. Lonzarich, and S. E. Sebastian, J. Phys.: Condens. Matter **21**, 012208 (2009).
[22] R. Hu, S. L. Budko, W. E. Straszheim, and P. C. Canfield, Phys. Rev. B **83**, 094520 (2011).